B-α/B-β Ring from Photosynthetic Complex LH4, Modeling of Absorption and Fluorescence Spectra

Pavel Heřman, David Zapletal

***Abstract*—**Absorption and steady state fluorescence spectra of B-α/B-β ring from the light-harvesting (LH) pigment-protein complex LH4 are investigated in this contribution. The geometric structure of some LH complexes is known in great detail, e.g. for the LH2 and LH4 complexes from purple bacteria. The properties of such complexes are strongly influenced by their interactions with environment. These interactions could be modeled by static and dynamic disorder. Different types of static disorder are considered and discussed. Resulting spectral profiles within full Hamiltonian model are presented and compared with our previous results within the nearest neighbour approximation model. Distribution of the quantity $P_\alpha d_\alpha^2$ that appears in the expression for steady state fluorescence spectrum is also studied. Comparison of the results for B-α/B-β ring from LH4 complex and B850 ring from LH2 complex is also done.

***Keywords*—**LH4, LH2, Absorption and fluorescence spectrum, Static and dynamic disorder

I. Introduction

In the process of photosynthesis (in plants, bacteria, and blue-green algae), solar energy is used to split water and produce oxygen molecules, protons and electrons. Photosynthesis is the process by which green plants and certain other organisms (bacteria, blue-green algae) transform light energy into chemical energy. During this process light energy is captured and used to convert water, carbon dioxide, and minerals into oxygen and energy-rich organic compounds. In chemical terms, photosynthesis is a light-energized oxidation-reduction process. Oxidation refers to the removal of electrons from a molecule; reduction refers to the gain of electrons by a molecule. These reactions occur in two stages: the light stage, consisting of photochemical (i.e., light-capturing) reactions; and the dark stage, comprising chemical reactions controlled by enzymes. During the first stage, the energy of light is absorbed and used to drive a series of electron transfers, resulting in the synthesis of ATP and the electron-donor reduced nicotine adenine dinucleotide phosphate (NADPH). During the dark stage, the ATP and NADPH formed in the light-capturing reactions are used to reduce carbon dioxide to organic carbon compounds [1].

From the energy point of view the major question is, how the solar energy can be used most effectively. Nowadays, the photovoltaic systems are wider used to harvest solar energy and transform it into electricity [2], [3]. But the disadvantage of this form of energy is problem with its storage. The solution of this problem could be to convert solar energy into chemical energy as hydrogen, which is easier to store than electricity. For this purpose, it is necessary to construct an effective artificial photosynthetic system [4]–[7]. Such system is not possible to be constructed without detailed knowledge of natural photosynthetic systems. The structure, properties and function of photosynthetic systems are the subject of investigation of many theoretical and experimental laboratories and research teams [8]–[13].

Our interest is mainly focused on first (light) stage of photosynthesis in purple bacteria. Solar photons are absorbed by a complex system of membrane-associated pigment-proteins (light-harvesting (LH) antenna) and the electronic excited state is efficiently transferred to a reaction center, where the light energy is converted into a chemical energy [14]. The antenna systems of photosynthetic units from purple bacteria are formed by ring units LH1, LH2, LH3, and LH4. The geometric structure is known in great detail from X-ray crystallography. The general organization of above mentioned light-harvesting complexes is the same: identical subunits are repeated cyclically in such a way that a ring-shaped structure is formed. However the symmetries of these rings are different.

Crystal structure of LH2 complex contained in purple bacterium *Rhodopseudomonas acidophila* was first described in high resolution by McDermott et al. [15], then further e.g. by Papiz et al. [16]. The bacteriochlorophyll (BChl) molecules are organized in two concentric rings. One ring features a group of nine well-separated BChl molecules (B800) with absorption band at about 800 nm. The other ring consists of eighteen closely packed BChl molecules (B850) absorbing around 850 nm. The whole

Manuscript received November , 2015.

This work was supported by the Faculty of Science, University of Hradec Králové (project of specific research No. 2105/2016 - P. Heřman).

P. Heřman is with the Department of Physics, Faculty of Science, University of Hradec Králové, Rokitanského 62, 50003 Hradec Králové, Czech Republic (e-mail: pavel.herman@uhk.cz).

D. Zapletal is with the Institute of Mathematics and Quantitative Methods, Faculty of Economics and Administration, University of Pardubice, Studentská 95, 53210 Pardubice, Czech Republic (e-mail: david.zapletal@upce.cz).

LH2 complex is nonameric, it consists of nine identical subunits. LH2 complexes from other purple bacteria have analogous ring structure.

Some bacteria contain also other types of complexes such as the B800-820 LH3 complex (*Rhodopseudomonas acidophila* strain 7050) or the LH4 complex (*Rhodopseudomonas palustris*). LH3 complex like LH2 one is usually nonameric but LH4 one is octameric (it consists of eight identical subunits). While the B850 dipole moments in LH2 ring have tangential arrangement, in the LH4 main B-α/B-β ring they are oriented more radially. In addition, mutual interactions of the nearest neighbour BChls in this LH4 ring are approximately two times smaller in comparison with B850 ring from LH2 complex and they have opposite sign. The other difference is the presence of two additional BChl rings in LH4 complex [17]. Different arrangements manifest themselves in different optical properties.

The intermolecular distances under 1 nm determine strong exciton couplings between corresponding pigments. That is why an extended Frenkel exciton states model could be used in theoretical approach. In spite of extensive investigation, the role of the protein moiety in governing the dynamics of the excited states has not been totally clear yet. At room temperature the solvent and protein environment fluctuate with characteristic time scales ranging from femtoseconds to nanoseconds. The simplest approach is to substitute fast fluctuations by dynamic disorder and slow fluctuations by static disorder.

Static disorder effect on the anisotropy of fluorescence for LH2 complexes was studied by Kumble and Hochstrasser [18] and Nagarajan et al. [19], [20]. We extended these investigations by consideration of dynamic disorder. We studied this effect for simple model systems [21]–[23] and then for models of B850 ring (from LH2) [24], [25]. Various types of uncorrelated static disorder (in local excitation energies, in transfer integrals, etc.) and correlated one (e.g., elliptical deformation) were used in the past [26]–[28] and also different arrangements of optical dipole moments were compared [29]–[32]. Recently we have focused on the modelling of absorption and steady state fluorescence spectra of LH2 and LH4 complexes within the nearest neighbour approximation model [33]–[37]. We have also extended our model to full Hamiltonian model and published the results for different types of static disorder [38], [40]–[43]. Very recently we have started to explore full LH2 complex (B850 ring and B800 ring) [44], [45].

Main goal of this paper is presentation of the steady state fluorescence and absorption spectra simulations for B-α/B-β ring from LH4 complex within full Hamiltonian model with static disorder in radial positions of molecules on the ring. The results are discussed and compared with our previous ones within the nearest neighbour approximation model. Comparison of the results calculated as for LH4 complex as for LH2 one for different types of static disorder is also done.

The rest of the paper is structured as follows. Section II introduces the ring model with static and dynamic disorder (interaction with phonon bath) and the cumulant expansion method, which is used for the calculation of spectral responses of the system with exciton-phonon coupling. Numerical consideration is mentioned in Section III, used units and parameters could be found in Section IV. Results of our simulations are presented and discussed in Section V and some conclusions are drawn in Section VI.

II. Model

The hamiltonian of an exciton in the ideal ring coupled to a bath of harmonic oscillators reads

$$H = H_{\rm ex}^0 + H_{\rm s} + H_{\rm ph} + H_{\rm ex-ph}. \tag{1}$$

First term,

$$H_{\rm ex}^0 = \sum_{m,n=1(m\neq n)}^{N} \bar{J}_{mn} a_m^\dagger a_n, \tag{2}$$

corresponds to an exciton, e.g. the system without any disorder. The operator $a_m^\dagger$ (a_m) creates (annihilates) an exciton at site m, $\bar{J}_{mn}$ (for $m \neq n$) is the so-called transfer integral between sites m and n. Inside one ring the pure exciton hamiltonian $H_{\rm ex}^0$ can be diagonalized using the wave vector representation with corresponding delocalized Bloch states α and energies E_α. Using Fourier transformed excitonic operators a_α, the Hamiltonian in α-representation reads

$$H_{\rm ex}^0 = \sum_{\alpha=1}^{N} E_\alpha a_\alpha^\dagger a_\alpha. \tag{3}$$

The interaction strengths between the nearest neighbour bacteriochlorophylls inside one subunit and between subunits are almost the same in B850 ring from LH2 complex (see Fig. 1 (B) in [17]). That is why this ring can be modeled as homogeneous case. If we consider the nearest neighbour approximation model (only the nearest neighbour transfer matrix elements are nonzero), we have

$$\bar{J}_{mn}^{\rm LH2} = J_0(\delta_{m,n+1} + \delta_{m,n-1}). \tag{4}$$

In this case the form of operators a_α is

$$a_\alpha = \sum_{n=1}^{N} a_n {\rm e}^{{\rm i}\alpha n}, \quad \alpha = \frac{2\pi}{N} l, \quad l = 0, \pm 1, \ldots, \pm\frac{N}{2}, \tag{5}$$

where $N = 18$ and the simplest exciton Hamiltonian for B850 ring from LH2 complex in α-representation is done by Eq. (3) with

$$E_\alpha^{\rm LH2} = -2J_0 \cos\alpha \tag{6}$$

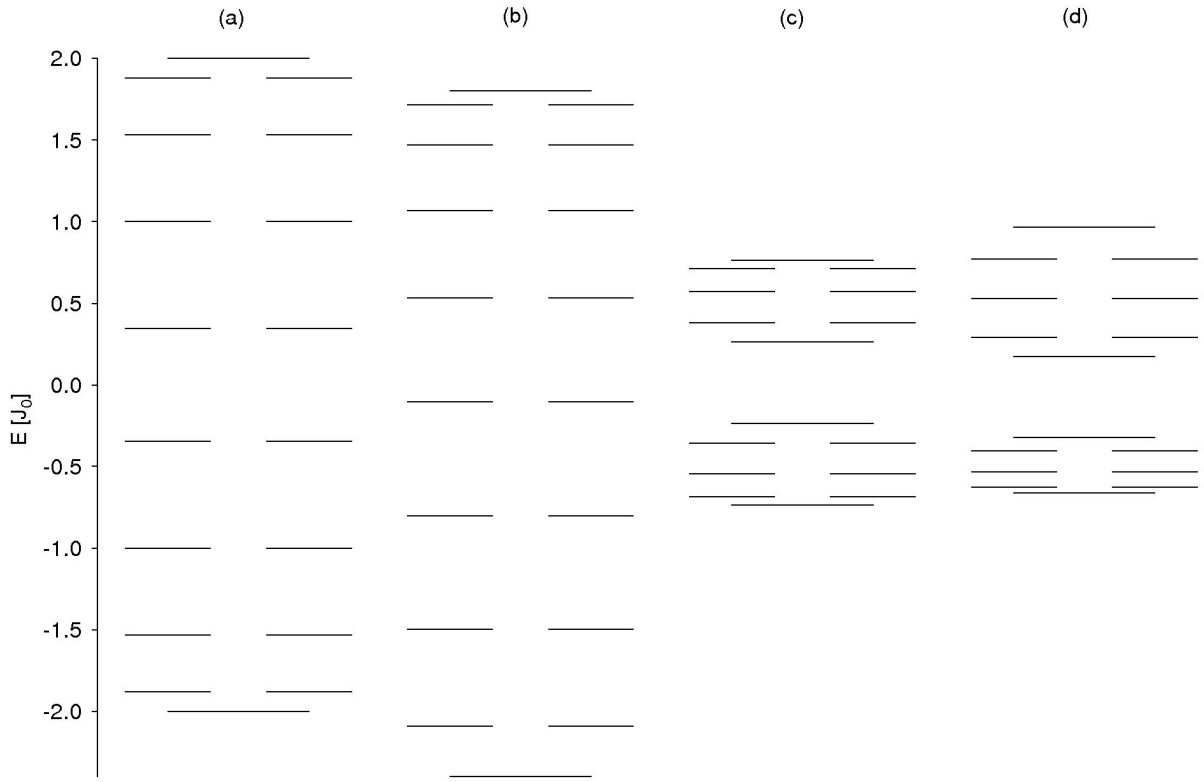

Fig. 1. Energetic band structures for B850 ring from LH2 complex ((a) – the nearest neighbour approximation model, (b) – full Hamiltonian model) and the same for B-α/B-β ring from LH4 complex ((c) – the nearest neighbour approximation model, (d) – full Hamiltonian model)

(see Figure 1 - column (a)).

B-α/B-β ring from LH4 complex consists of 16 BChls ($N = 16$) and it is considerably dimerized (interaction strength between the nearest neighbour bacteriochlorophylls inside one subunit is approximately two times higher in comparison with that between subunits (see Fig. 1 (A) in [17]). If the nearest neighbour approximation is taken into account, transfer matrix elements read

$$\bar{J}_{mn}^{\mathrm{LH4}} = -J_0 \left(\frac{\delta_{m,n+1}}{2} + \frac{\delta_{m,n-1}}{4} \right) \tag{7}$$

for odd m and

$$\bar{J}_{mn}^{\mathrm{LH4}} = -J_0 \left(\frac{\delta_{m,n+1}}{4} + \frac{\delta_{m,n-1}}{2} \right) \tag{8}$$

for even m. That is why energetic spectrum of B-α/B-β ring from LH4 complex is different from that of B850 ring from LH2 complex (see Figure 1 - column (c)).

If we consider full Hamiltonian model with dipole-dipole approximation, transfer integrals J_{mn} can be written as

$$J_{mn} = \frac{\vec{d}_m \cdot \vec{d}_m}{|\vec{r}_{mn}|^3} - 3\frac{\left(\vec{d}_m \cdot \vec{r}_{mn}\right)\left(\vec{d}_n \cdot \vec{r}_{mn}\right)}{|\vec{r}_{mn}|^5} = \tag{9}$$

$$= |\vec{d}_m||\vec{d}_n| \frac{\cos\varphi_{mn} - 3\cos\varphi_m \cos\varphi_n}{|\vec{r}_{mn}|^3}. \tag{10}$$

Here $\vec{d_m}$ and $\vec{d_n}$ are local dipole moments of m-th and n-th molecule respectively, $\vec{r}_{mn}$ is the vector connecting m-th and n-th molecule and φ_m (φ_n) is angle between $\vec{d}_m$ ($\vec{d}_n$) and $\vec{r}_{mn}$. Angle between m-th and n-th vector of local dipole moment ($\vec{d}_m$, $\vec{d}_n$) is referred to as φ_{mn}. In dipole-dipole approximation geometric arrangement of the ring has to correspond with the interaction strengths between the nearest neighbour bacteriochlorophylls. That is why distances $r_{m,m+1}$ of neighbouring molecules in B850 ring from LH2 complex are the same (without any disorder) and angles $\beta_{m,m+1}$ have to be the same too ($\beta_{m,m+1} = 2\pi/18$, see Figure 2). On the other hand, dimerization is present in B-α/B-β ring from LH4 complex. Therefore distances $r_{m,m+1}$ and angles $\beta_{m,m+1}$ (see Figure 3) are different and have to correspond to different interaction strengths (see Eq. (7) and Eq. (8)). In this case energetic band structures slightly differ from that for the nearest neighbour approximation model. For B850 ring from LH2 complex the differences of energies in lower part of the band are higher and in upper part of the band are smaller in comparison with the nearest neighbour approximation model (see Figure 1 - column (b)). On the other hand, differences of the energies in lower part of the band are smaller and in upper part of the band are higher for B-α/B-β ring from LH4 complex (see Figure 1 - column (d)).

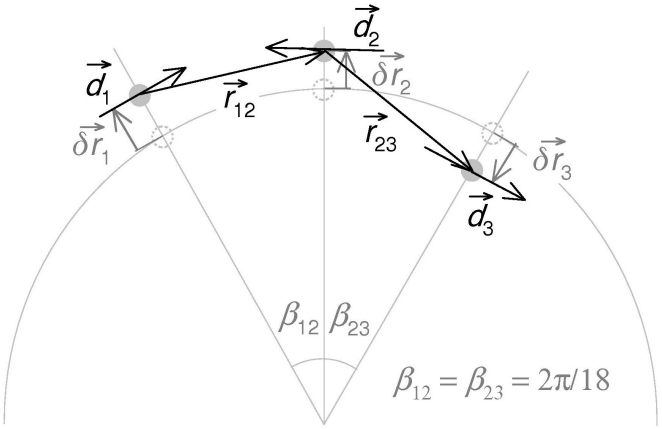

Fig. 2. Fluctuations in radial positions of molecules δr_k – B850 ring from LH2 complex

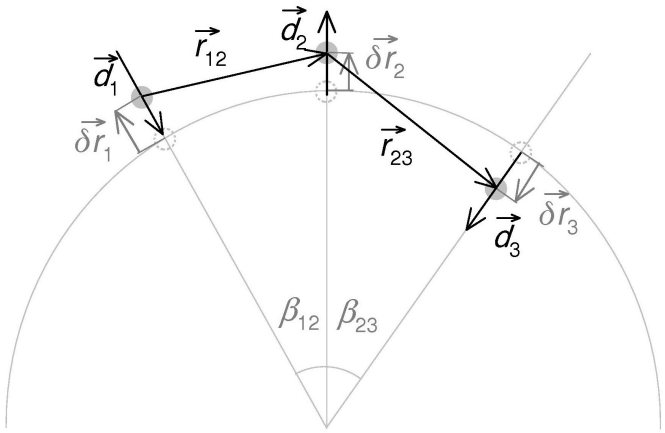

Fig. 3. Fluctuations in radial positions of molecules δr_k – B-α/B-β ring from LH4 complex

The second term in Eq. (1), $H_{\rm s}$, corresponds to static disorder. Influence of static disorder is modeled by uncorrelated fluctuations of radial positions of molecules δr_k on the ring (with Gaussian distribution and standard deviation Δ_r),

$$r_k = r_0 + \delta r_k, \tag{11}$$

where r_0 is the radial position of molecules without any disorder. Fluctuations δr_k manifest themselves in fluctuations of transfer integrals J_{mn} but with the distribution different from Gaussian one [27]. The third term in Eq. (1),

$$H_{\rm ph} = \sum_q \hbar\omega_q b_q^\dagger b_q, \tag{12}$$

represents phonon bath in the harmonic approximation. The phonon creation and annihilation operators are denoted by $b_q^\dagger$ and b_q, respectively.

Last term,

$$H_{\rm ex-ph} = \frac{1}{\sqrt{N}} \sum_m \sum_q G_q^m \hbar\omega_q a_m^\dagger a_m (b_q^\dagger + b_q), \tag{13}$$

describes exciton-phonon interaction which is assumed to be site-diagonal and linear in the bath coordinates (the term G_q^m denotes the exciton-phonon coupling constant).

For the calculation of spectral responses of the system with exciton-phonon coupling we use the cumulant-expansion method of Mukamel et al. [46]. We can express absorption $OD(\omega)$ and steady-state fluorescence $FL(\omega)$ spectra as

$$OD(\omega) = \omega \sum_\alpha d_\alpha^2 \times$$
$$\times {\rm Re} \int_0^\infty dt {\rm e}^{{\rm i}(\omega-\omega_\alpha)t - g_{\alpha\alpha\alpha\alpha}(t) - R_{\alpha\alpha\alpha\alpha}t}, \tag{14}$$

$$FL(\omega) = \omega \sum_\alpha P_\alpha d_\alpha^2 \times$$
$$\times {\rm Re} \int_0^\infty dt {\rm e}^{{\rm i}(\omega-\omega_\alpha)t + {\rm i}\lambda_{\alpha\alpha\alpha\alpha}t - g^*_{\alpha\alpha\alpha\alpha}(t) - R_{\alpha\alpha\alpha\alpha}t}. \tag{15}$$

Here

$$\vec{d}_\alpha = \sum_n c_n^\alpha \vec{d}_n \tag{16}$$

is the transition dipole moment of eigenstate α, c_n^α are the expansion coefficients of the eigenstate α in site representation and P_α is the steady state population of the eigenstate α. The inverse lifetime of exciton state $R_{\alpha\alpha\alpha\alpha}$ is given by the elements of Redfield tensor [47] (a sum of the relaxation rates between exciton states)

$$R_{\alpha\alpha\alpha\alpha} = -\sum_{\beta\neq\alpha} R_{\beta\beta\alpha\alpha}. \tag{17}$$

The g-functions and λ-values in Eq. (15) are given by

$$g_{\alpha\beta\gamma\delta} = -\int_{-\infty}^{\infty} \frac{d\omega}{2\pi\omega^2} C_{\alpha\beta\gamma\delta}(\omega) \times$$
$$\times \left[\coth\frac{\omega}{2k_{\rm B}T}(\cos\omega t - 1) - {\rm i}(\sin\omega t - \omega t) \right], \tag{18}$$

$$\lambda_{\alpha\beta\gamma\delta} = -\lim_{t\to\infty} \frac{d}{dt} {\rm Im}\{g_{\alpha\beta\gamma\delta}(t)\} =$$
$$= \int_{-\infty}^{\infty} \frac{d\omega}{2\pi\omega} C_{\alpha\beta\gamma\delta}(\omega). \tag{19}$$

The matrix of the spectral densities $C_{\alpha\beta\gamma\delta}(\omega)$ in the eigenstate (exciton) representation reflects the coupling of one-exciton states to the manifold of nuclear modes. In what follows, only a diagonal exciton phonon interaction in site representation is used (see Eq. (13)), i.e., only fluctuations of the pigment site energies are assumed and the restriction to the completely uncorrelated dynamical disorder is applied. In such case each site (i.e. each chromophore) has its own bath completely uncoupled from the baths of the other sites. Furthermore, it is

assumed that these independent baths have identical properties

$$C_{mnm'n'}(\omega) = \delta_{mn}\delta_{mm'}\delta_{nn'}C(\omega). \tag{20}$$

After transformation to exciton representation we have

$$C_{\alpha\beta\gamma\delta}(\omega) = \sum_n c_n^\alpha c_n^\beta c_n^\gamma c_n^\delta C(\omega). \tag{21}$$

Several models of spectral density of the bath are used in literature [48]–[50]. It is not entirely clear, which model gives the best description of phonon bath in case of ring antenna complexes as LH2 and LH4. In our present investigation we have used the model of Kühn and May [49]

$$C(\omega) = \Theta(\omega) j_0 \frac{\omega^2}{2\omega_c^3} \mathrm{e}^{-\omega/\omega_c}, \tag{22}$$

which has its maximum at $2\omega_c$.

III. Numerical Considerations

To obtain absorption and steady state fluorescence spectra, it is necessary to calculate single ring $OD(\omega)$ and $FL(\omega)$ spectra for large number of different static disorder realizations created by random number generator. Finally, these results have to be averaged over all realizations of static disorder.

For our previous calculations of absorption and steady state fluorescence spectra (with Gaussian uncorrelated static disorder in local excitation energies δE_n and in transfer integrals δJ_{mn} taking into account) software package Mathematica [51] was used. Standard numerical integration method used in Mathematica proved to be unsuitable in case of full Hamiltonian model and static disorder δr_n in radial positions of molecules. It was not possible to achieve satisfactory convergence by above mentioned integration method from Mathematica. This is the reason a procedure in Fortran was created for present calculations.

Integrated functions are oscillating and damped (see Eq. (14) and Eq. (15)) and function $\mathrm{Re}\, g_{\alpha\alpha\alpha\alpha}(t)$ is non-negative. Therefore absolute values of integrated functions (for individual α) satisfy inequalities

$$\left|\mathrm{Re}\left\{\mathrm{e}^{\mathrm{i}(\omega-\omega_\alpha)t - g_{\alpha\alpha\alpha\alpha}(t) - R_{\alpha\alpha\alpha\alpha}t}\right\}\right| \leq \mathrm{e}^{-R_{\alpha\alpha\alpha\alpha}t}, \tag{23}$$

$$\left|\mathrm{Re}\left\{\mathrm{e}^{\mathrm{i}(\omega-\omega_\alpha)t + \mathrm{i}\lambda_{\alpha\alpha\alpha\alpha}t - g^*_{\alpha\alpha\alpha\alpha}(t) - R_{\alpha\alpha\alpha\alpha}t}\right\}\right| \leq \mathrm{e}^{-R_{\alpha\alpha\alpha\alpha}t}. \tag{24}$$

The whole $OD(\omega)$ and $FL(\omega)$ then satisfy

$$OD(\omega) \leq \omega \sum_{\alpha=1}^{N} d_\alpha^2 \int_0^\infty dt\, \mathrm{e}^{-R_{\alpha\alpha\alpha\alpha}t}, \tag{25}$$

$$FL(\omega) \leq \omega \sum_{\alpha=1}^{N} P_\alpha d_\alpha^2 \int_0^\infty dt\, \mathrm{e}^{-R_{\alpha\alpha\alpha\alpha}t} \leq$$

$$\leq \omega \sum_{\alpha=1}^{N} d_\alpha^2 \int_0^\infty dt\, \mathrm{e}^{-R_{\alpha\alpha\alpha\alpha}t}. \tag{26}$$

Predetermined accuracy could be achieved by integration over finite time interval $t \in \langle 0, t_0\rangle$ (instead of $\langle 0, \infty\rangle$). If

$$t_0 \geq \max\{t_\alpha\}, \quad \alpha = 1, \ldots, N, \tag{27}$$

where t_α satisfies condition

$$d_\alpha^2 \left[\int_0^\infty dt\, \mathrm{e}^{-R_{\alpha\alpha\alpha\alpha}t} - \int_0^{t_\alpha} dt\, \mathrm{e}^{-R_{\alpha\alpha\alpha\alpha}t}\right] =$$

$$= d_\alpha^2 \frac{\mathrm{e}^{-R_{\alpha\alpha\alpha\alpha}t_\alpha}}{R_{\alpha\alpha\alpha\alpha}} \leq \frac{Q}{N\omega}, \tag{28}$$

i.e.

$$t_\alpha \geq \frac{1}{R_{\alpha\alpha\alpha\alpha}} \ln\left(\frac{N\omega d_\alpha^2}{Q R_{\alpha\alpha\alpha\alpha}}\right), \tag{29}$$

then deviations of $OD(\omega)$ and $FL(\omega)$ from precise values are not larger then Q. Here Q is arbitrary real positive number and $N = 18$ for B850 ring from LH2 complex or $N = 16$ for B-α/B-β ring from LH4 complex. $OD(\omega)$ and $FL(\omega)$ are therefore integrated as sums of contributions from individual cycles of oscillation. These contributions are added until upper limit of integration exceeds t_0.

IV. Units and Parameters

Dimensionless energies normalized to the transfer integral $\bar{J}_{1,2}^{\mathrm{LH2}} = J_0$ in B850 ring from LH2 complex (see Eq. (4)) have been used in our simulations. Estimation of J_0 varies in literature between 250 cm^{-1} and 400 cm^{-1}. The nearest neighbour transfer integrals in B-α/B-β ring (LH4) have opposite sign in comparison with those in B850 ring (LH2). Furthermore, dimerization can be found in LH4 complex in contrast with LH2 complex [17] and that is why the transfer integrals in B-α/B-β ring (LH4) differ from those in B850 ring (LH2) also in their absolute values (see Eq. (7) and Eq. (8)). Therefore we have taken the values of the nearest neighbour transfer integrals in B-α/B-β ring from LH4 complex as follows:

$$\bar{J}_{12}^{LH4} = -0.5\bar{J}_{12}^{LH2} = -0.5J_0,$$

$$\bar{J}_{23}^{LH4} = 0.5\bar{J}_{12}^{LH4} = -0.25J_0.$$

In our previous investigations [52] we found from comparison with experimental results for B850 ring from LH2 complex [53] that the possible strength of the uncorrelated static disorder in radial positions of molecules Δ_r is approximately $\Delta_r \approx 0.06\ r_0$. That is why we have taken the strengths Δ_r = 0.01, 0.02, 0.04, 0.06, 0.08 r_0. In case of fluctuations in transfer integrals δJ_{mn} we suppose that the strength of static disorder

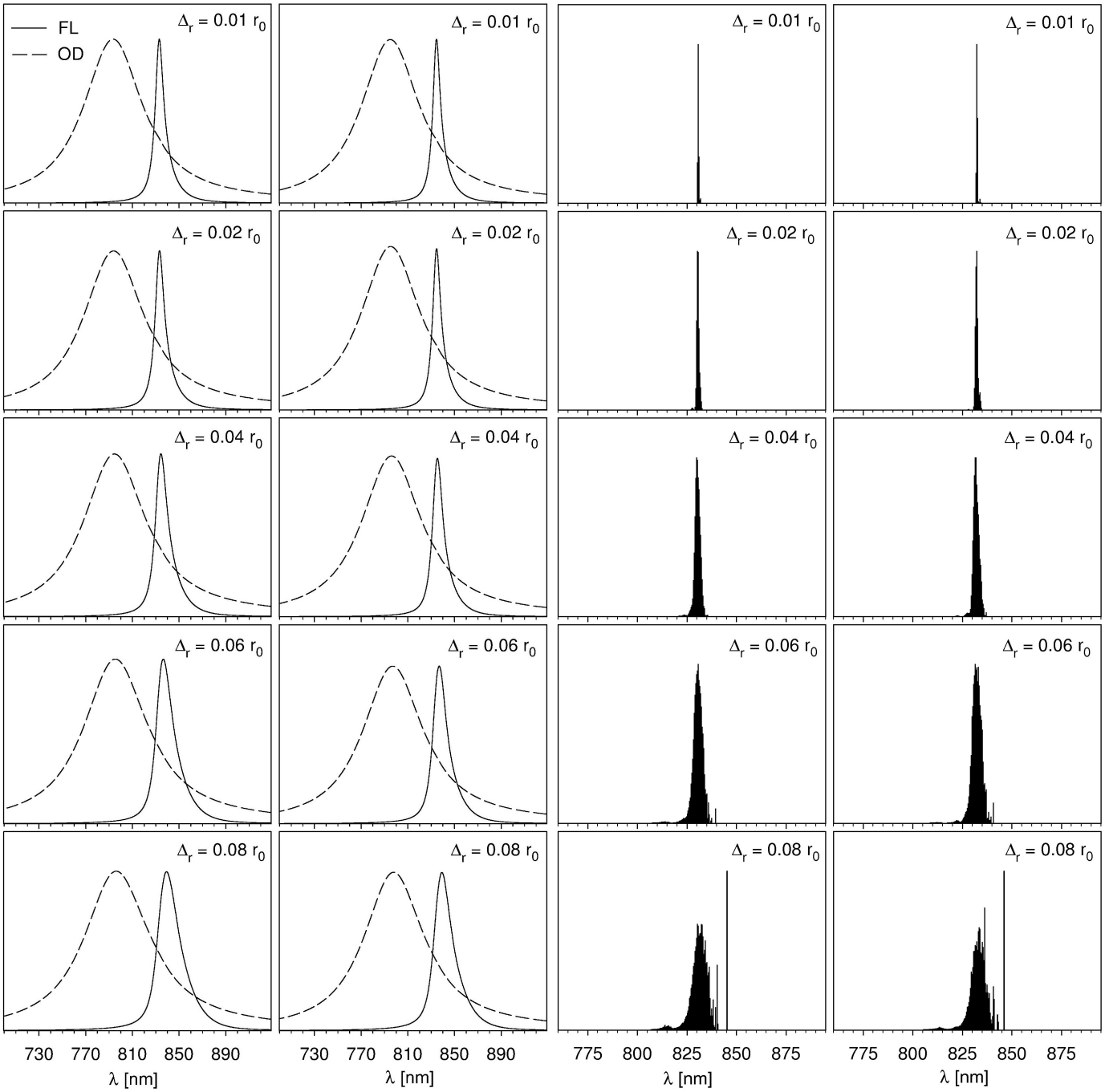

Fig. 4. Calculated $FL(\omega)$ and $OD(\omega)$ spectra of B-α/B-β ring from LH4 complex averaged over 2000 realizations of Gaussian uncorrelated static disorder in radial positions of molecules δr_k (low temperature $kT = 0.1\ J_0$, five strengths Δ_r of static disorder) and related distributions of the quantity $P_\alpha d_\alpha^2$ as a function of wavelengths. First and third column – full Hamiltonian model, second and fourth column – the nearest neighbour approximation model

is proportional to absolute value of respective transfer integral $\bar{J}_{mn}$ in the ideal ring (without any disorder)

$$J_{mn} = \bar{J}_{mn}\left(1 + \frac{\delta J_{mn}}{\bar{J}_{mn}}\right). \tag{30}$$

We have taken the strength of static disorder Δ_J = 0.225, 0.250, 0.275, 0.300, 0.325 $\bar{J}_{mn}$.

For the best reproduction of experimental data for LH2 complex [48] within the nearest neighbour approximation model and static disorder in radial positions of molecules on the ring, our previous investigations give the following values of interpigment interaction energy J_0 and unperturbed transition energy from the ground state E_0:

$$J_0 = 400\ \mathrm{cm}^{-1}, \quad E_0 = 12350\ \mathrm{cm}^{-1}.$$

In order to compare the results for both models of

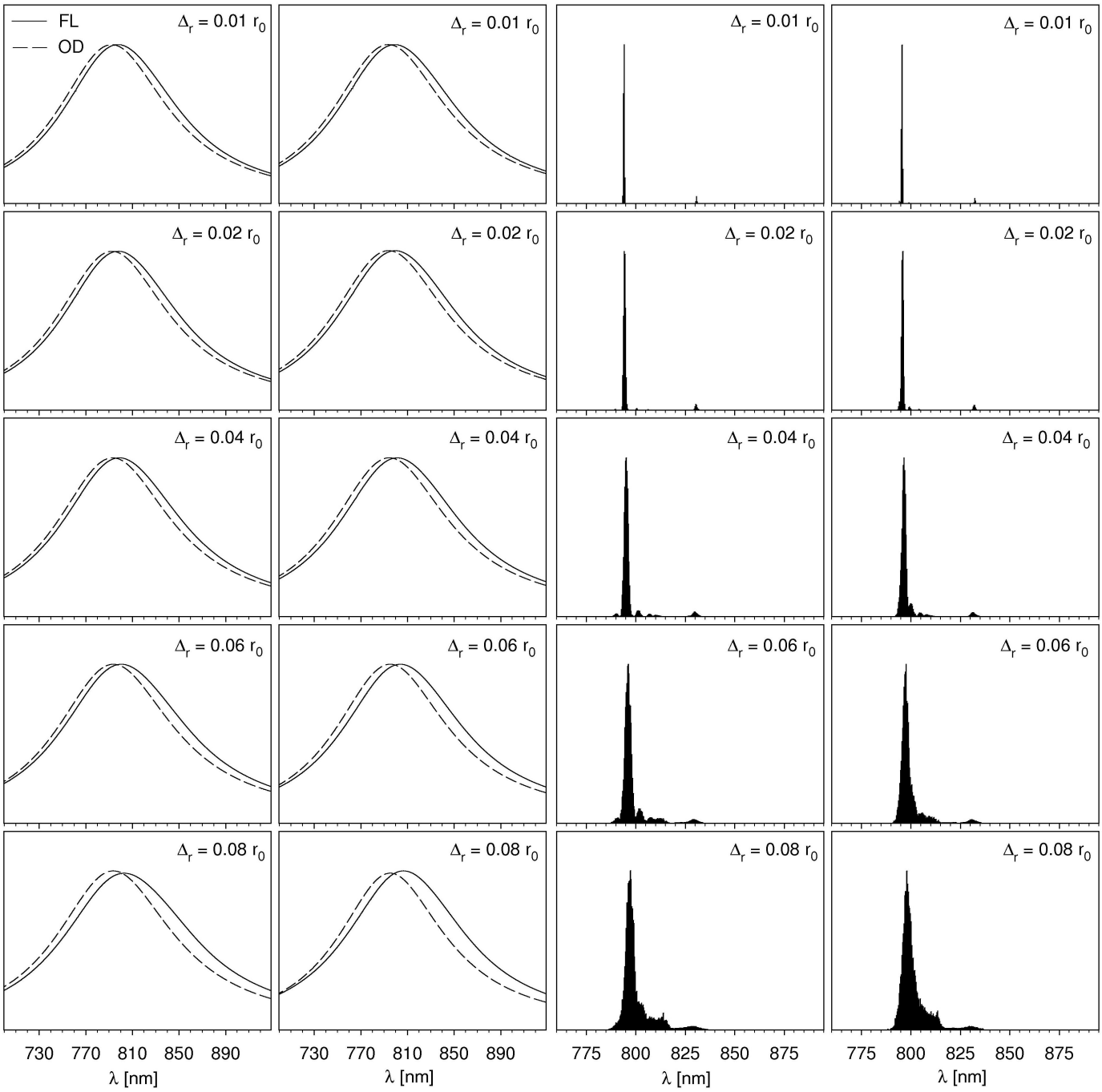

Fig. 5. Calculated $FL(\omega)$ and $OD(\omega)$ spectra of B-α/B-β ring from LH4 complex averaged over 2000 realizations of Gaussian uncorrelated static disorder in radial positions of molecules δr_k (room temperature $kT = 0.5\ J_0$, five strengths Δ_r of static disorder) and related distributions of the quantity $P_\alpha d_\alpha^2$ as a function of wavelengths. First and third column – full Hamiltonian model, second and fourth column – the nearest neighbour approximation model

Hamiltonian, we have done the simulations for full Hamiltonian model with the same values J_0 and E_0. As concerns spectral density function $C(\omega)$, we have used the model of Kühn and May [49] (see Eq. (22)) with values of the parameters j_0 and ω_c chosen in agreement with our previous results [28]:

$$j_0 = 0.4 J_0, \quad \omega_c = 0.212 J_0.$$

V. Results and Discussion

Novoderezhkin et al. studied LH2 complex [48] but only for room temperature and for one type of uncorrelated static disorder (fluctuations of local excitation energies). We did similar calculations for B850 ring from LH2 complex with the same type of static disorder (fluctuations of local excitation energies) as for the nearest neighbour approximation model (NN)as for

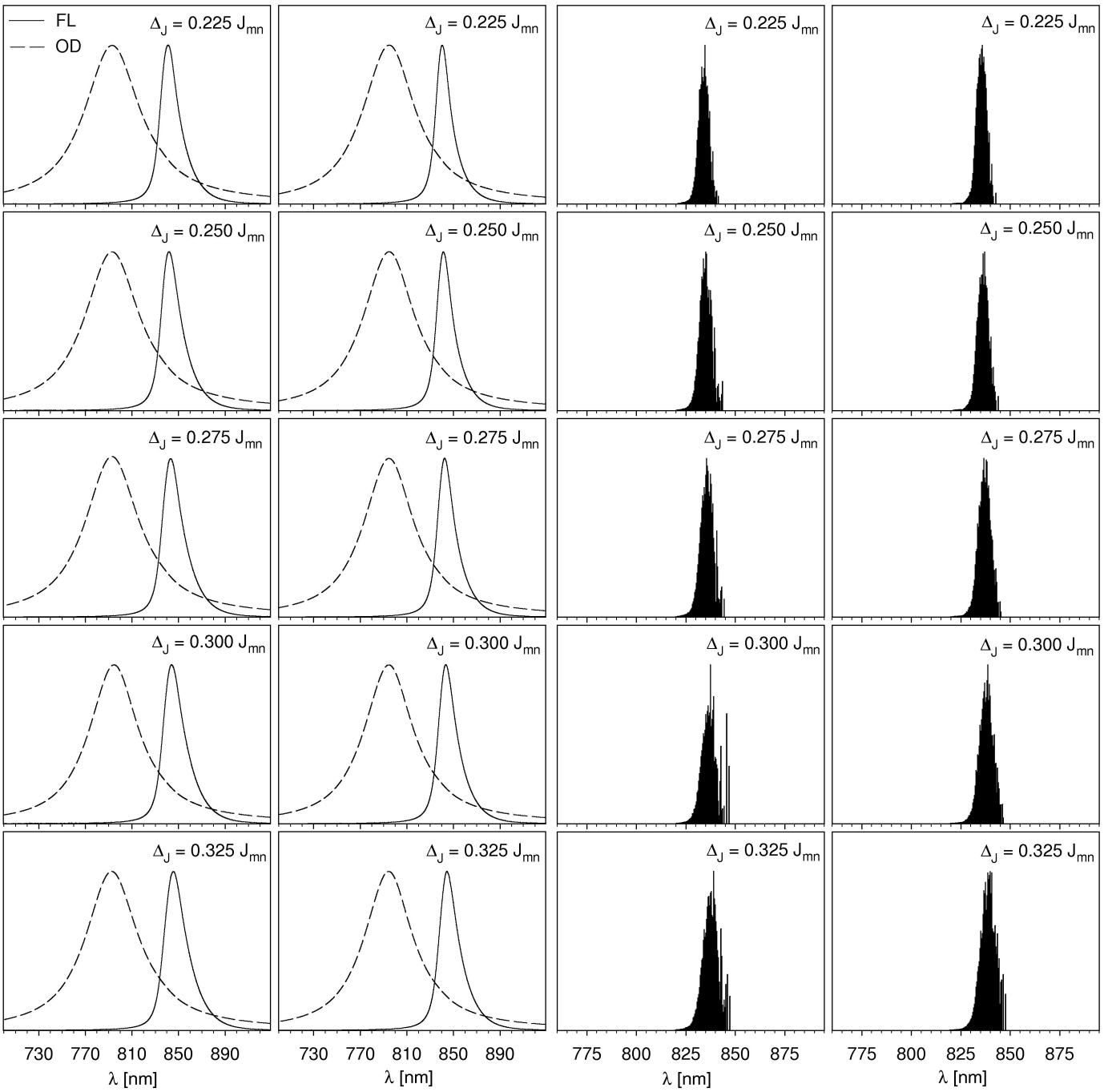

Fig. 6. Calculated $FL(\omega)$ and $OD(\omega)$ spectra of B-α/B-β ring from LH4 complex averaged over 2000 realizations of Gaussian uncorrelated static disorder in transfer integrals δJ_{mn} (low temperature $kT = 0.1\ J_0$, five strengths Δ_J of static disorder) and related distributions of the quantity $P_\alpha d_\alpha^2$ as a function of wavelengths. First and third column – full Hamiltonian model, second and fourth column – the nearest neighbour approximation model

full Hamiltonian model (FH) but also for low temperature [34], [38]. Besides this type of static disorder we also used other types of static disorder (uncorrelated fluctuations δJ_{mn} of transfer integrals and uncorrelated fluctuations δr_m of radial positions of molecules on the ring [34], [41]). In addition, the spectral density function $C(\omega)$ (see Eq. (22)) which differs from that one used by Novoderezhkin et al. [48] was taken into account in our simulations. Previous results for LH4 complex were published e.g. by Ruijter et al. [17] (fluorescence spectrum) and Read et al. [54] (absorption spectrum) for low temperature. Again we did calculations for NN model as for low temperature as for room temperature and for three above mentioned types of static disorder [35], [37], [42]. The results for FH model and fluctuations in local excitation energies $\delta\varepsilon_n$ and transfer

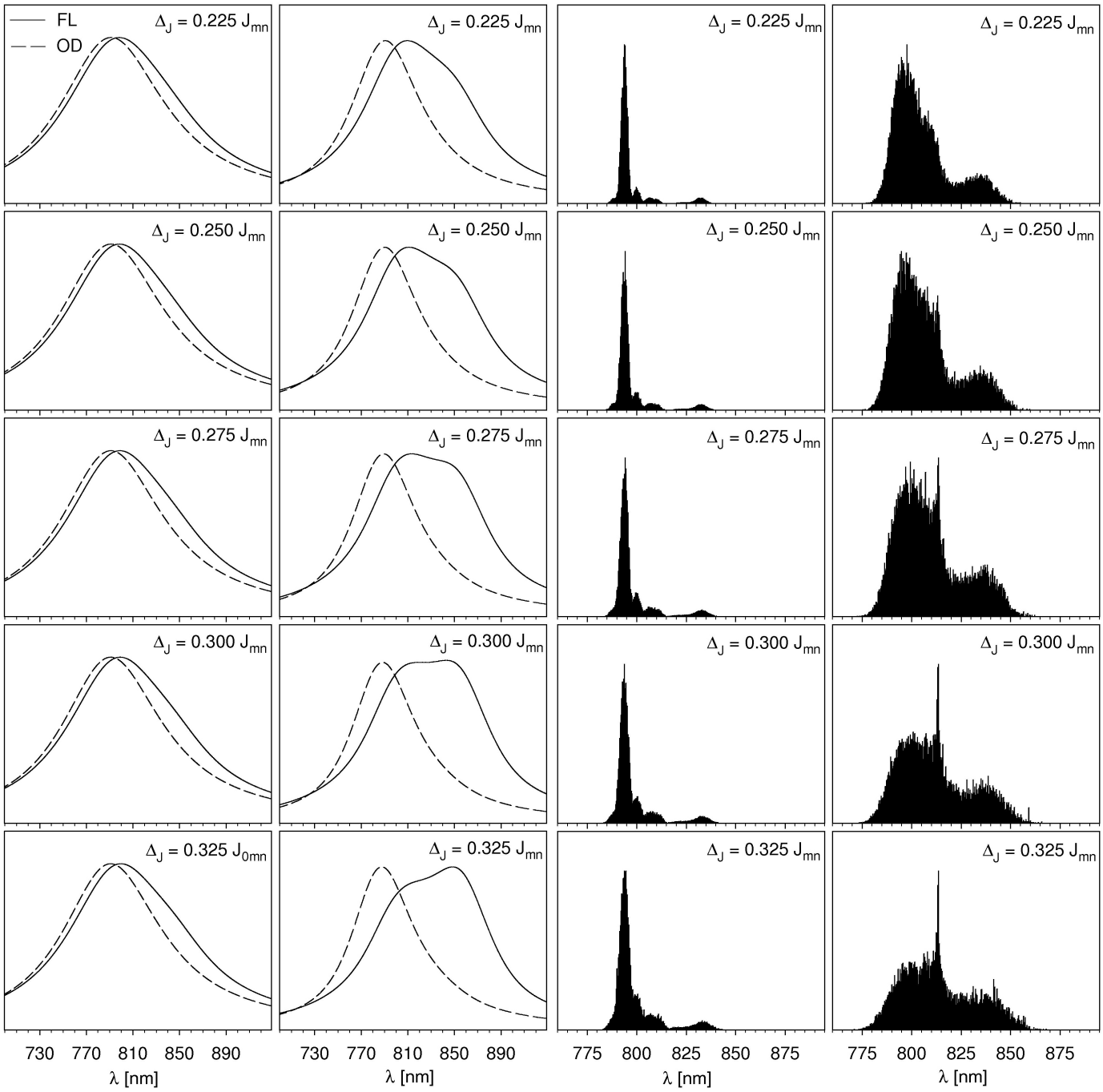

Fig. 7. Calculated $FL(\omega)$ and $OD(\omega)$ spectra of B-α/B-β ring from LH4 complex averaged over 2000 realizations of Gaussian uncorrelated static disorder in transfer integrals δJ_{mn} (room temperature $kT = 0.5\ J_0$, five strengths Δ_J of static disorder) and related distributions of the quantity $P_\alpha d_\alpha^2$ as a function of wavelengths. First and third column – full Hamiltonian model, second and fourth column – the nearest neighbour approximation model

integrals δJ_{mn} were published in [39], [40]. New results for B-α/B-β ring from LH4 complex within FH model and Gaussian uncorrelated static disorder δr_k in radial positions of molecules on the ring are presented in this paper. Also comparison with our previous results from different viewpoints is done.

Absorption spectra $OD(\omega)$ and steady state fluorescence spectra $FL(\omega)$ of B-α/B-β ring from LH4 complex averaged over 2000 realizations of Gaussian uncorrelated static disorder δr_k in radial positions of molecules on the ring for low temperature $kT = 0.1\ J_0$ can be seen in Figure 4 (first and second column) and for room temperature $kT = 0.5\ J_0$ in Figure 5 (first and second column). The same, but for uncorrelated Gaussian static disorder in transfer integrals δJ_{mn}, is drawn in Figure 6 (first and second column) and in Figure 7

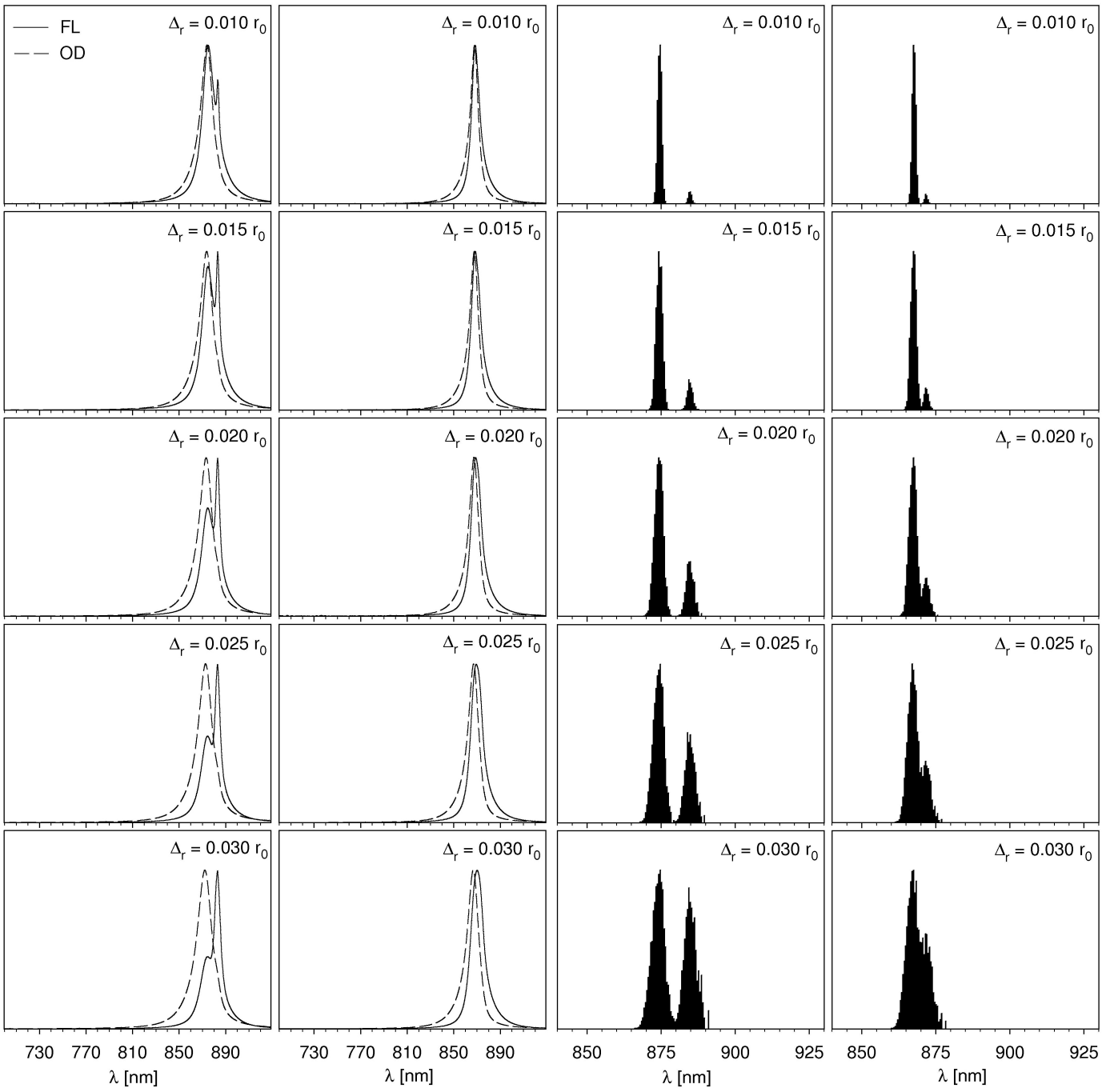

Fig. 8. Calculated $FL(\omega)$ and $OD(\omega)$ spectra of B850 ring from LH2 complex averaged over 2000 realizations of Gaussian uncorrelated static disorder in radial positions of molecules δr_k (low temperature $kT = 0.1\ J_0$, five strengths Δ_r of static disorder) and related distributions of the quantity $P_\alpha d_\alpha^2$ as a function of wavelengths. First and third column – full Hamiltonian model, second and fourth column – the nearest neighbour approximation model

(first and second column). Absorption and steady state fluorescence spectra ($OD(\omega)$ and $FL(\omega)$) of B850 ring from LH2 complex with the same type of static disorder (fluctuations δr_k in radial positions of molecules on the ring) for low temperature $kT = 0.1\ J_0$ are shown in Figure 8 (first and second column) and for room temperature $kT = 0.5\ J_0$ in Figure 9 (first and second column).

At low temperature ($kT = 0.1\ J_0$) the steady state fluorescence spectra $FL(\omega)$ of B850 ring from LH2 complex substantially differ for FH model and for NN one. Fluorescence spectral line splitting is visible in FH model contrary to NN model. These differences are visible for all three types of static disorder: fluctuations in radial positions of molecules δr_n (Figure 8 - first and second column), fluctuations in local excitation energies

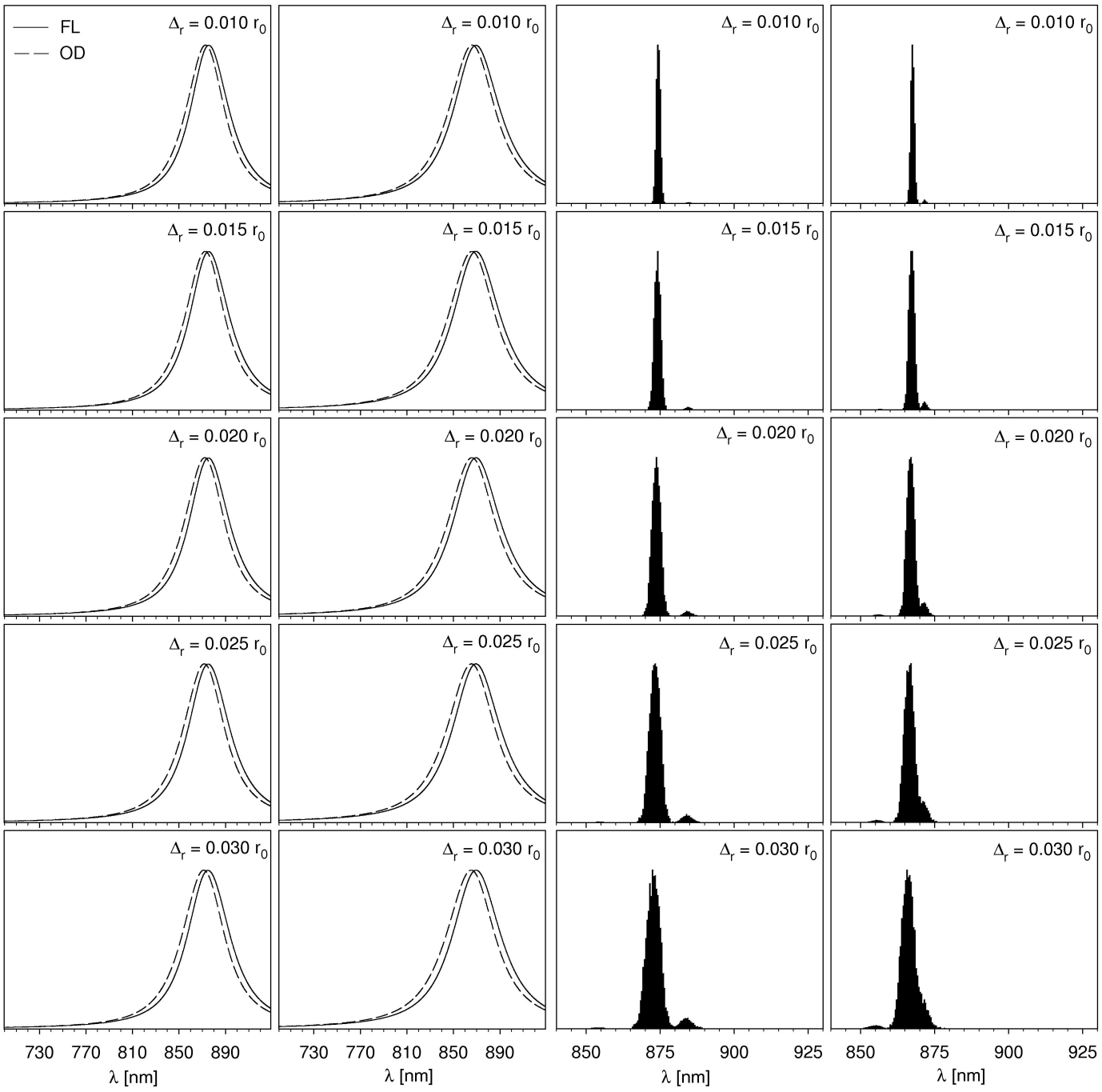

Fig. 9. Calculated $FL(\omega)$ and $OD(\omega)$ spectra of B850 ring from LH2 complex averaged over 2000 realizations of Gaussian uncorrelated static disorder in radial positions of molecules δr_k (room temperature $kT = 0.5\ J_0$, five strengths Δ_r of static disorder) and related distributions of the quantity $P_\alpha d_\alpha^2$ as a function of wavelengths. First and third column – full Hamiltonian model, second and fourth column – the nearest neighbour approximation model

$\delta\varepsilon_n$ [38], fluctuations in transfer integrals δJ_{mn} [41]. At room temperature $kT = 0.5\ J_0$ fluorescence spectra for FH model and for NN one are qualitatively same - only one peak appears.

The situation is different in case of B-α/B-β ring from LH4 complex. The indication of fluorescence spectral line splitting is visible for NN model (contrary to FH model in LH2), but only for room temperature $kT = 0.5\ J_0$. These differences are visible only for static disorder in transfer integrals δJ_{mn} (Figure 7 - first and second column) and for static disorder in local excitation energies $\delta\varepsilon_n$ [40]. In case of fluctuations in radial positions δr_n of molecules, the fluorescence spectrum $FL(\omega)$ has only one peak for both models of Hamiltonian (NN and FH), as for low temperature $kT = 0.1\ J_0$ (see Figure (4)) as for room temperature

$kT = 0.5\ J_0$ (see Figure (5)).

For clarification of the fluorescence spectral line splitting appearance, the distributions of the quantity $P_\alpha d_\alpha^2$ have been investigated. Here P_α is the steady state population of the eigenstate α and d_α^2 is the dipole strength of the eigenstate α (see Eq. (15)). Corresponding distributions of this quantity as a function of wavelength λ can be seen in Figure 4 – Figure 9 (third and fourth column). The distributions correspond to fluorescence spectral profiles $FL(\omega)$. The differences in $FL(\omega)$ spectra between B850 ring from LH2 complex and B-α/B-β ring from LH4 complex are caused by different energetic band structures (see Figure 1) and especially by different optically active states. Without any disorder, the optically active states in case of B-α/B-β ring from LH4 complex are two upper states (with the same energy) just below the highest state (see Figure 1 – columns (c) and (d)). On the other hand, the optically active states in B850 ring from LH2 complex are two lower states ($\alpha = \pm 1$) just above the lowest state (see Figure 1 – columns (a) and (b)). If static disorder is present, also other states became optically active.

The distribution of $P_\alpha d_\alpha^2$ has only one peak (around 830$\sim$835 nm) for LH4 ring at low temperature. But the second peak (around 795 nm) arises at room temperature . This second peak totally prevails in case of fluctuations in radial positions of molecules δr_n (for both models of Hamiltonian). Therefore fluorescence spectrum has only one peak as for low temperature as for room temperature for this type of static disorder. On the other hand, the second peak is not so dominant for other types of static disorder ($\delta\varepsilon_n$ and δJ_{mn}), especially for FH model. That is why, the fluorescence spectral line splitting is visible, but only for room temperature. For LH2 ring, at least a hint of two peaks in distributions of $P_\alpha d_\alpha^2$ appears for both temperatures and both models of Hamiltonian. But the distance and height of the peaks are different. For FH model the positions of the peaks are approximately at 8750 nm (higher peak) and 885 nm (lower peak) and the dominance of higher peak is not so critical at low temperature. Therefore the splitting of fluorescence spectrum is visible in this case. For NN model the distance of the peaks in $P_\alpha d_\alpha^2$ distributions is approximately two times lower (868 nm - higher peak, 872 nm - lower peak). The peaks are mutually almost overlapped in this case and only one peak appears in $FL(\omega)$ spectral profiles.

As concerns absorption spectra $OD(\omega)$, both models of Hamiltonian and all types of static disorder give substantially the same results. Only comparison of $OD(\omega)$ spectra for low and room temperature brings significant difference in spectral width. Absorption spectra are substantially wider for room temperature in comparison with low temperature.

VI. Conclusions

Comparison of the results obtained within different models of Hamiltonian and different types of static disorder can be summarized as follows. The most essential difference, spectral line splitting, appears in fluorescence spectra. This effect has different reasons for different types of LH complexes. In case of B850 ring from LH2 complex the splitting is caused by the substitution of NN Hamiltonian model by FH one, but the splitting is not significantly influenced by changing of static disorder type. On the other hand, fluorescence spectral line splitting depends mainly on static disorder type for B-α/B-β ring from LH4 complex. The appearance of this effect is not substantially affected by the model of Hamiltonian in this case. These differences lie in different energetic band structures and different optically active states of these photosynthetic complexes.

References

[1] D. W. Lawlor, *Photosynthesis*. New York: Springer, 2001.

[2] A. A. Bayod-Rújula,A. Ortego-Bielsa, A. Martínez-Gracia, "Photovoltaics on flat roofs: Energy considerations", *Energy* 36, 2011, pp. 1996–2010.

[3] R. E. Blankenship, D. M. Tiede, J. Barber, G. W. Brudvig, G. Fleming, M. Ghirardi, M. R. Gunner, W. Junge, D. M. Kramer, A. Melis, "Comparing the efficiency of photosynthesis with photovoltaic devices and recognizing opportunities for improvement", *Science* 332, 2011, pp. 805–809.

[4] Y. Sun, Ch. Liu, D. C. Grauer, J. Yano, J. R. Long, P. Yang, J. Ch. Chang, "Electrodeposited cobalt-sulfide catalyst for electrochemical and photoelectrochemical hydrogen generation from water", *J. Am. Chem. Soc.* 135, 2013, pp. 17699–17702.

[5] K. Kalyanasundaram, M. Graetzel, "Artificial photosynthesis: biomimetic approaches to solar energy conversion and storage", *Current Opinion in Biotechnology* 21, 2010, pp. 298-310.

[6] L. Savage, "Saving solar energy for a rainy day: Artificial photosynthesis", *Optics and Photonics News* 24(2), 2013, pp. 18–25.

[7] T. Faunce, "Towards a global solar fuels project- Artificial photosynthesis and the transition from anthropocene to sustainocene", *Procedia Engineering* 49, 2012, pp. 348-356.

[8] E. Sorgüven, M. Özilgen, "Thermodynamic efficiency of synthesis, storage and breakdown of the high-energy metabolites by photosynthetic microalgae", *Energy* 58, 2013, pp. 679–687.

[9] H. M. Amaro, A. C. Macedo, F. X. Malcata, "Microalgae: An alternative as sustainable source of biofuels?", *Energy* 44, 2012, pp. 158–166.

[10] A. Bahadar, M. B. Khan, "Progress in energy from microalgae: A review", *Renew. and Sustain. En. Rev.* 27, 2013, pp. 128–148.

[11] A. W. D. Larkum, "Limitations and prospects of natural photosynthesis for bioenergy production", *Curr. Opin. Biotech.* 21, 2010, pp. 271–276.

[12] R. Petela, "An approach to the exergy analysis of photosynthesis", *Sol. En.* 82, 2008, pp. 311–328.

[13] V. H. Work, S. DAdamo, R. Radakovits, R. E. Jinkerson, M. C. Posewitz, "Improving photosynthesis and metabolic networks for the competitive production of phototroph-derived biofuels", *Curr. Opin. Biotech.* 23, 2012, pp. 290–297.

[14] R. van Grondelle, V. I. Novoderezhkin, "Energy transfer in photosynthesis: experimental insights and quantitative models", *Phys. Chem. Chem. Phys.* 8, 2003, pp. 793–807.

[15] G. McDermott, S. M. Prince, A. A. Freer, A. M. Hawthornthwaite-Lawless, M. Z. Papiz, R. J. Cogdell, N. W. Isaacs, "Crystal structure of an integral membrane light-harvesting complex from photosynthetic bacteria", *Nature* 374, 1995, pp. 517–521.

[16] M. Z. Papiz, S. M. Prince, T. Howard, R. J. Cogdell, N. W. Isaacs, "The structure and thermal motion of the B 800850 LH2 complex from Rps. acidophila at 2.0 A resolution and 100 K: new structural features and functionally relevant motions", *J. Mol. Biol.* 326, 2003, pp. 1523–1538.

[17] W. P. F. de Ruijter, S. Oellerich, J.-M. Segura, A. M. Lawless, M. Papiz, T. J. Aartsma, "Observation of the Energy-Level Structure of the Low-Light Adapted B800 LH4 Complex by Single-Molecule Spectroscopy", *Biophys. J.* 87, 2004, pp. 3413–3420.

[18] R. Kumble, R. Hochstrasser, "Disorder-induced exciton scattering in the light-harvesting systems of purple bacteria: Influence on the anisotropy of emission and band → band transitions", *J. Chem. Phys.* 109, 1998, pp. 855–865.

[19] V. Nagarajan, E. T. Johnson, J. C. Williams, W. W. Parson, "Femtosecond pump-probe spectroscopy of the B850 antenna complex of Rhodobacter sphaeroides at room temperature", *J. Phys. Chem. B* 103, 1999, pp. 2297–2309.

[20] V. Nagarajan, W. W. Parson, "Femtosecond fluorescence depletion anisotropy: Application to the B850 antenna complex of Rhodobacter sphaeroides", *J. Phys. Chem. B* 104, 2000, pp. 4010–4013.

[21] V. Čápek, I. Barvík, P. Heřman, "Towards proper parametrization in the exciton transfer and relaxation problem: dimer", *Chem. Phys.* 270, 2001, pp. 141–156.

[22] P. Heřman, I. Barvík, "Towards proper parametrization in the exciton transfer and relaxation problem. II. Trimer", *Chem. Phys.* 274, 2001, pp. 199–217.

[23] P. Heřman, I. Barvík, M. Urbanec, "Energy relaxation and transfer in excitonic trimer", *J. Lumin.* 108, 2004, pp. 85–89.

[24] P. Heřman, U. Kleinekathöfer, I. Barvík, M. Schreiber, "Exciton scattering in light-harvesting systems of purple bacteria", *J. Lumin.* 94-95, 2001, pp. 447–450.

[25] P. Heřman, I. Barvík, "Non-Markovian effects in the anisotropy of emission in the ring antenna subunits of purple bacteria photosynthetic systems", *Czech. J. Phys.* 53, 2003, pp. 579–605.

[26] P. Heřman, U. Kleinekathöfer, I. Barvík, M. Schreiber, "Influence of static and dynamic disorder on the anisotropy of emission in the ring antenna subunits of purple bacteria photosynthetic systems", *Chem. Phys.* 275, 2002, pp. 1–13.

[27] P. Heřman, I. Barvík, "Temperature dependence of the anisotropy of fluorescence in ring molecular systems", *J. Lumin.* 122–123, 2007, pp. 558–561.

[28] P. Heřman, D. Zapletal, I. Barvík, "Computer simulation of the anisotropy of fluorescence in ring molecular systems: Influence of disorder and ellipticity", *Proc. IEEE 12th Int. Conf. on Computational Science and Engineering*, Vancouver: IEEE Comp. Soc., 2009, pp. 437–442.

[29] P. Heřman, I. Barvík, "Coherence effects in ring molecular systems", *Phys. Stat. Sol. C* 3, 2006, 3408–3413.

[30] P. Heřman, D. Zapletal, I. Barvík, "The anisotropy of fluorescence in ring units III: Tangential versus radial dipole arrangement", *J. Lumin.* 128, 2008, pp. 768–770.

[31] P. Heřman, I. Barvík, D. Zapletal, "Computer simulation of the anisotropy of fluorescence in ring molecular systems: Tangential vs. radial dipole arrangement", *Lecture Notes in Computer Science* 5101, 2008, pp. 661–670.

[32] P. Heřman, D. Zapletal, I. Barvík, "Loss of coherence due to disorder im molecular rings", *Phys. Stat. Sol. C* 6, 2009, pp. 89–92.

[33] P. Heřman, D. Zapletal, J. Šlégr, "Comparison of emission spectra of single LH2 complex for different types of disorder", *Phys. Proc.* 13, 2011, pp. 14–17.

[34] D. Zapletal, P. Heřman, "Simulation of molecular ring emission spectra: localization of exciton states and dynamics", *Int. J. Math. Comp. Sim.* 6, 2012, pp. 144–152.

[35] M. Horák, P. Heřman, D. Zapletal, "Simulation of molecular ring emission spectra - LH4 complex: localization of exciton states and dynamics", *Int. J. Math. Comp. Sim.* 7, 2013, pp. 85–93.

[36] M. Horák, P. Heřman, D. Zapletal, "Modeling of emission spectra for molecular rings - LH2, LH4 complexes", *Phys. Proc.* 44, 2013, pp. 10–18.

[37] P. Heřman, D. Zapletal, "Intermolecular coupling fluctuation effect on absorption and emission spectra for LH4 ring", *Int. J. Math. Comp. Sim.* 7, 2013, pp. 249–257.

[38] P. Heřman, D. Zapletal, M. Horák, "Emission spectra of LH2 complex: full Hamiltonian model", *Eur. Phys. J. B* 86, 2013, art. no. 215.

[39] P. Heřman, D. Zapletal, "Emission Spectra of LH4 Complex: Full Hamiltonian Model", *Int. J. Math. Comp. Sim.* 7, 2013, pp. 448–455.

[40] P. Heřman, D. Zapletal, "Simulation of Emission Spectra for LH4 Ring: Intermolecular Coupling Fluctuation Effect", *Int. J. Math. Comp. Sim.* 8, 2014, pp. 73–81.

[41] D. Zapletal, P. Heřman, "Photosynthetic complex LH2 - Absorption and steady state fluorescence spectra", *Energy* 77, 2014, pp. 212–219.

[42] P. Heřman, D. Zapletal, "Simulations of emission spectra for LH4 ring - Fluctuations of radial positions of molecule", *Int. J. Biol. Biomed. Eng.* 9, 2015, pp. 65–74.

[43] P. Heřman, D. Zapletal, "Computer Simulation of Emission and Absorption Spectra for LH2 Ring", *Computational Problems in Science and Engineering, Lecture Notes in Electrical Engineering* 343, 2015.

[44] P. Heřman, D. Zapletal, "Modeling of Absorption and Steady State Fluorescence Spectra of Full LH2 Complex (B850 - B800 Ring)", *International Journal of Mathematical Models and Methods in Applied Sciences* 9, 2015, pp. 614–623.

[45] P. Heřman, D. Zapletal, "Modeling of emission and absorption spectra of LH2 complex (B850 and B800 ring) - full Hamiltonian model", *Int. J. Math. Comp. Sim.* 10, 2016, pp. 208–217.

[46] S. Mukamel, *Principles of nonlinear optical spectroscopy*. New York: Oxford University Press, 1995.

[47] A. G. Redfield, "The Theory of Relaxation Processes", *Adv. Magn. Reson.* 1, 1965, pp. 1–32.

[48] V. I. Novoderezhkin, D. Rutkauskas, R. van Grondelle, "Dynamics of the emission spectrum of a single LH2 complex: Interplay of slow and fast nuclear motions", *Biophys. J.* 90, 2006, pp. 2890–2902.
complexes from *Rhodopseudomonas acidophila* strain 10050", *Biochemistry* 43, 2004, pp. 4431–4438.

[49] V. May, O. Kühn, *Charge and Energy Transfer in Molecular Systems*. Berlin: Wiley-WCH, 2000.

[50] O. Zerlauskiene, G. Trinkunas, A. Gall, B. Robert, V. Urboniene, "Static and Dynamic Protein Impact on Electronic Properties of Light-Harvesting Complex LH2", *J. Phys. Chem. B* 112, 2008, pp. 15883–15892.

[51] S. Wolfram, *The Mathematica Book*. Wolfram Media, 2003.

[52] P. Heřman, I. Barvík, D. Zapletal, "Energetic disorder and exciton states of individual molecular rings", *J. Lumin.* 119-120, 2006, pp. 496–503.

[53] C., Hofmann, T. J. Aartsma, J. Kőhler, "Energetic disorder and the B850-exciton states of individual light-harvesting 2 complexes from Rhodopseudomonas acidophila", *Chem. Phys. Lett.* 395, 2004, pp. 373–378.

[54] E. L. Read, G. S. Schlau-Cohen, G. S. Engel, T. Georgiou, M. Z. Papiz, G. R. Fleming, "Pigment organization and energy level structure in light-harvesting complex 4: Insights from two-dimensional electronic spectroscopy", *J. Phys. Chem. B*, 113, 2009, pp. 6495–6504.